Journal of the Serbian Chemical Society
JSCS-info@shd.org.rs • www.shd.org.rs/JSCS
J. Serb. Chem. Soc. *85* (9) 1197–1221 (2020)
JSCS–5369
UDC 544.773.432+547.995.15:544.4:544.14:536.2
Original scientific paper

Thermo-responsive hydrogels based on poly(*N*-isopropylacrylamide) and hyaluronic acid cross-linked with nanoclays

ILINKA MIRKOVIĆ[1], MARIJA S. NIKOLIĆ[1#], SANJA OSTOJIĆ[2], JELENA MALETAŠKIĆ[3], ZORAN PETROVIĆ[4] and JASNA DJONLAGIĆ[1*#]

[1]Faculty of Technology and Metallurgy, University of Belgrade, Karnegijeva 4, Belgrade, Serbia, [2]Institute of General and Physical Chemistry, University of Belgrade, Studentski trg 12–16, Belgrade, Serbia, [3]Vinča Institute of Nuclear Sciences, Materials Science Laboratory, University of Belgrade, Belgrade, Serbia and [4]Kansas Polymer Research Center, Pittsburg State University, Pittsburg, KS, 66762, USA

(Received 9 January 2019, revised 30 March, accepted 2 May 2020)

Abstract: Semi-interpenetrating polymer networks (SIPN) based on thermo-responsive poly(*N*-isopropylacrylamide) (PNIPA) and water-soluble sodium salts of linear hyaluronic acid (Na-HA) were physically cross-linked with synthetic nanoclay (laponite XLG). PNIPA hydrogels with different cross-linking densities and Na-HA concentrations were synthesized by *in situ* free-radical redox polymerization. The structure and heterogeneity of the semi-IPN hydrogels were examined by SEM and XRD. The content of clay incorporated in the gel was determined by TGA. DSC measurements showed that volume phase transition temperature and its enthalpy varied with the clay and hyaluronic acid content. SIPN hydrogels containing negatively charged polyelectrolyte, Na-HA, exhibited higher Q_e and faster deswelling rates than the corresponding PNIPA NC hydrogels. The presence of the anionic Na-HA polymer reduced the storage modulus, indicating a weakening of the hydrogel network structure, especially at lower clay contents. The nanocomposite hydrogels exhibited high tan δ values, which increased with increasing Na-HA content.

Keywords: thermo-responsive hydrogels; semi-IPN hydrogels; nanoclay; hyaluronic acid; swelling/deswelling kinetics.

INTRODUCTION

Polymer hydrogels that respond to external chemical and physical stimuli, with a large and reversible volume change have been widely studied from scientific and technical perspectives in the past several decades. Elastic and high water content polymer hydrogels resemble natural living tissue and have great

* Corresponding author. E-mail: jasna@tmf.bg.ac.rs
# Serbian Chemical Society member.
https://doi.org/10.2298/JSC200109023M

potential as biomaterials for a large number of the pharmaceutical and biotechnological applications.[1–3] Thermally responsive hydrogels based on cross-linked poly(*N*-isopropylacrylamide) (PNIPA) exhibit a reversible volume phase transition temperature (*VPTT*) within the physiological temperature range, close to 32––34 °C.[4] However, their low response rate and low strength limited their use. In 2002, Haraguchi *et al.*[5–7] reported on thermo-responsive nanocomposite (NC) hydrogels based on PNIPA and layered silicates that exhibited high transparency, high swelling/deswelling rates and excellent mechanical properties compared to traditional, chemically cross-linked PNIPA hydrogels. The NC hydrogels were synthesized by free radical polymerization of *N*-isopropylacrylamide (NIPA) monomer in an aqueous suspension of synthetic clay, hectorite laponite XLG. Laponite belongs to the 2:1 phyllosilicates with an octahedral layer surrounded by two tetrahedral layers. The exfoliated thin disk-like clay platelets (*ca*. 1 nm thickness and 30 nm in diameter) in water, carrying negative charge on the surface and positive charge at the edge, acted as multifunctional physical cross-linkers with large effective functionality. It was reported that the average effective functionality (N_{eff}) per one clay particle increased from 50 to 165 with increasing clay and monomer concentration.[6,8–11] Generally, the interaction between the clay platelets and attached PNIPA chains to their surface is considered as a combination of ionic interaction and hydrogen bonding.[6]

Many strategies for preparing thermo-responsive PNIPA-based hydrogels with improved mechanical and rapid swelling/deswelling response have been investigated. They included the formation of semi-interpenetrating networks by addition of a high-molar mass linear polymer to the primary cross-linked network (SIPNs).[12–14] For example, NC reinforced SIPN PNIPA hydrogels with linear hydrophilic poly(*N*-vinyl pyrolidone) (PVP) showed improved mechanical properties and thermal responsiveness.[13] The addition of high-molar mass linear PVP polymer chains introduced entanglements and reinforced the network. PVP also affected the polymer–solvent interactions and changed the responsiveness of hydrogels. In addition, linear, hydrophilic and nonionic poly(vinyl alcohol) (PVA) was used to enhance the rate and level of thermal response of PNIPA NC hydrogels, and to impart good chemical resistance, processability, biocompatibility, and biodegradability.[14–16] SIPN NC hydrogels with dual temperature and pH responses have been prepared by using linear poly(acrylic acid) (PAA),[17,18] carboxymethylcellulose (CMC)[19,20] or carboxymethylchitosan (CMCS).[21] PNIPA hydrogels for biomedical application are often used in aqueous or physiological media and therefore, the mechanical, thermal, and other physical properties in both the as-prepared and swollen state are of significant importance.[11,22]

Hyaluronic acid (HA), also known as hyaluronan, is a high molar mass polysaccharide, *i.e.*, glycosaminoglycan, consisting of multiple disaccharide repeating units of D-glucuronic acid and *N*-acetyl-D-glucosamine linked *via* β(1–3) and

β(1–4) glycoside bonds. Hyaluronan is a semi-flexible and negatively charged biopolymer, with one carboxylate group per disaccharide repeating unit, which adopts a stiffened, wormlike chain conformation in aqueous solutions.[23,24] Hyaluronic acid is a natural component of the extracellular matrix of various connective tissues in humans and animals. HA plays an important role in many biological processes, such as tissue hydration, nutrient diffusion, proteoglycan organization and cell differentiation, as well as in tissue regeneration.[25] Due to its good biocompatibility, biodegradability, excellent gel-forming properties, HA is good candidate for biomedical applications to create patches for fast wound healing and tissue regeneration, as well as drug release systems.

Only a few studies related to the synthesis of PNIPA hydrogels with hyaluronic acid (HA) were found in the reviewed literature. Coronado *et al.*[26] reported the synthesis of semi-IPN, consisting of chemically cross-linked PNIPA hydrogels with 1, 2 and 3 wt. % HA. A potential application was injectable and non-toxic biomaterial. Santos *et al.*[27] showed that the introduction of HA into PNIPA--based semi-IPN improved drug (gentamicin) release of the hydrogels due to the accelerated swelling/deswelling transition. Recently, double chemically cross-linked IPN hydrogels based on hyaluronic acid/poly(*N*-isopropylacrylamide) (HA/ /PNIPA) for transdermal delivery of luteolin were reported.[28] Cytotoxicity tests measured on the eluate from HA/PNIPA hydrogels confirmed that there was no toxicity, which is essential for their application to the skin. Despite the significant potential of PNIPA hydrogels in biomedical application, hitherto there have been some concerns in the scientific community regarding their local toxicity. It is known that NIPA monomer is toxic and therefore, it is essential to have a comprehensive understanding of the cytotoxicity and biosafety of PNIPA hydrogels. Recently, a few papers comprehensively addressed cytotoxicity, genotoxicity, and proliferation tests using several cell lines.[29–32] Biocompatibility studies of PNIPA hydrogels verified by different techniques showed that the material is non-cytotoxic and non-genotoxic.[29] A comprehensive study on the cytotoxicity of NIPA monomer, PNIPA polymer and PNPA films on four different mammalian cell lines reported that the purity of the polymer is essential for a non-cytotoxic response.[31] In addition, some *in vivo* experiments (rabbits) confirmed that intravitreal injections of PNIPA solution were nontoxic.[33] On the other hand, mild toxicity of PNIPA hydrogels *in vitro* and *in vivo* (mouse) was reported, which was attributed to the release of residual monomers and impurities from commercially available PNIPA hydrogel.[34] Therefore, it was established that purified PNIPA polymers and hydrogels could be considered as biocompatible materials.

The objective of this study was to develop high strength, physically cross--linked, thermo-responsive hydrogels modified by an ionically-charged natural polymer with improved responsiveness, and to study their structure–property

relationships. Three series of semi-IPNs based on water-soluble high molar mass sodium hyaluronate (Na-HA) and thermo-responsive PNIPA physically cross--linked with inorganic clay (hectorite, laponite XLG) were developed. The hydrogels were synthesized by free radical polymerization in aqueous media with different cross-linking densities by varying the content of clay from 1 to 5 wt. %. In order to obtain semi-IPN polymer networks, hydrogels were synthesized in the presence of 0.1; 0.15 and 0.25 wt. % the anionic polyelectrolyte, Na-HA. For comparison, a series of pure PNIPA hydrogels reinforced with laponite XLG nanoclay with the corresponding clay content was prepared.

The responsiveness of the gels was estimated from the equilibrium swelling at 25 °C and swelling/deswelling kinetics. The morphology of freeze-dried gel samples was examined with a scanning electron microscope (SEM). The gel structure and heterogeneity were analyzed by X-ray diffraction (XRD) analysis. The thermal stabilities of the gels and their clay content were investigated by thermogravimetric (TG) analysis. The thermo-sensitive response of hydrogels was studied by differential scanning calorimetry (DSC). The rheological properties of the prepared hydrogels in the as-prepared and equilibrium swollen state were tested by dynamic mechanical analysis (DMA).

EXPERIMENTAL

Materials

N-Isopropylacrylamide (NIPA, Acros Organics, New Jersey, USA) was purified by recrystallization from a cyclohexane/toluene (60/40 volume ratio) mixture and dried under vacuum at 40 °C. Synthetic hectorite, laponite XLG ($[Mg_{5.34}Li_{0.66}Si_8O_{20}(OH)_4]Na_{0.66}$ from Rockwood, Ltd., TX, USA, was used as purchased. The layer diameter was 20–30 nm and thickness of 1 nm; cation exchange capacity (*CEC*), 104 meq per 100 g of clay and sodium counter ions). Ammonium peroxodisulfate (APS) as the redox initiator was recrystallized from water. The sodium salt of hyaluronic acid (Na-HA, 95.2 %), M_w, 1.16×10^6 g mol^{-1}, glucuronic acid content 45.6 % and pH 6.6 (Zhejiang Lide Biochemical, China), and accelerator, *N*,*N*,*N*′,*N*′-tetramethylethylenediamine (TEMED) (Sigma–Aldrich) were used as received.

Synthesis of NC hydrogels

The NC hydrogels were synthesized by *in situ* free-radical redox polymerization. The molar concentration of NIPA monomer (1.0 mol dm^{-3}) was the same for all samples. The clay concentrations were 1, 3 and 5 wt. %. The hydrogels were designated as PNIPA-C*x*, where *x* is the weight percent of clay.

NC hydrogels were prepared according to the procedure reported in a previous paper, with slight modifications.[13] As a typical example, the hydrogel PNIPA-C3 was prepared by adding 2.26 g (0.02 mol) of NIPA and 0.6 g of synthetic clay in 19.8 mL of distilled water and stirred under nitrogen flow at 900 rpm at room temperature. The reaction mixture was bubbled with nitrogen for 60 min to remove residual oxygen. Then, the reaction mixture was cooled to around 2 °C in an ice-bath. Then 0.2 mL of a 10 wt. % freshly prepared solution of APS initiator was added and 5.4 μL of accelerator, TEMED, was injected. The polymerization was performed at room temperature for 24 h in glass molds (12.5 cm×12.5 cm glass plates separated by a 2.0 mm thick rubber gasket). After polymerization, the hydrogel sheets were taken

from glass molds and one part was stored in the as-prepared state. The other part of the hydrogels was soaked in an excess of distilled water for at least 4 days, with daily refreshment to remove residual unreacted monomer.

Semi-IPN hydrogels were prepared in the same manner at three Na-HA concentrations (0.1, 0.15 and 0.25 wt. % of Na-HA), with the addition of the desired amount of the clay. Na-HA solutions were prepared by mixing the appropriate amount of polymer and water at room temperature under stirring (500–800 rpm) until the polymer was completely dissolved. Then, clay (0.20–1.00 g) was added to the Na-HA solution (19.8 ml) by stirring at room temperature for 1–3 h until the mixed aqueous dispersion became homogeneous. Three series of SIPNs were labeled as: SIPN-HA*z*-C*y*, where *y* represents the weight content of clay and *z* the weight percent of Na-HA in the solution. The sample composition and designations of NC hydrogels are presented in Table I later on.

Characterization of NC hydrogels

X-Ray diffraction (XRD) analysis of the powder of clay Laponite XLG and the powder of milled dried NC gels was performed with aqn Ultima IV Rigaku X-ray diffractometer. Scanning was carried out at 2θ from 2 to 30° (step scan: 0.50 s, step width: 0.02°) in a Bragg–Brentano geometry using CuK_α radiation (λ = 0.15418 nm). The operating voltage was 40 kV and the current 30 mA.

The morphology of the NC gels was examined with field emission scanning electron microscopy (FESEM, Mira3 Tescan) at an accelerating voltage of 10 kV. To conserve the microstructure of the hydrogel without collapse, the samples for this analysis were frozen and subsequently freeze-dried for 24 h under vacuum at –40 °C. In order to observe the interior morphology, the freeze-dried samples were carefully cut with scalpel after immersion in liquid nitrogen. Finally, the samples were coated with gold to a thickness of *ca.* 5 nm prior to the SEM observation. The average pore sizes and their distributions were determined from the SEM micrographs using ImageJ 1.38x software, based on 200 measurements per sample.

The swelling kinetics of NC hydrogels were monitored gravimetrically on the as-prepared round-shaped specimens. The hydrogel disks (2.5 mm thick and diameter of 1 cm) were immersed in distilled water (for at least four days at 25 °C) to remove the residual monomer, and then dried to constant weight. The dried samples were placed in distilled water at 25 °C and weighed after different periods during swelling. The average value of five measurements was used for each sample. The degree of swelling, Q, was calculated as the ratio of the weight of the hydrogel specimen swollen at time t, W_t, and the weight of the dry gel, W_d.

The kinetics of deswelling was followed gravimetrically at 40 °C with hydrogel samples previously swollen to equilibrium in distilled water at 25 °C. The weight changes of the hydrogels were recorded at different times during the deswelling process. Deswelling kinetics of hydrogels was followed through changes in water retention (WR) defined as:

$$WR = \frac{W(H_2O)_t}{W(H_2O)_e} \quad (1)$$

where W_t and W_e are the weights of water in the hydrogel at time t and in the equilibrium swollen state, respectively.

Thermogravimetric (TG) analysis was realized on TA Instruments, SDT Q600, USA, in order to evaluate the extent of the incorporation of clay. The amount of remaining clay in xerogel was measured after one cycle of swelling/deswelling. Hydrogel disks were placed in distilled water at least 4 days and then dried until constant weight. The xerogel samples were

heated from 30 to 800 °C in air (flow rate of 100 mL min^{-1}) at a heating rate of 20 °C min^{-1}. The clay content in the dried NC xerogels was calculated from the residual weight at 770 °C.

Differential scanning calorimetery (DSC) was performed on TA Instruments, model Q1000, Delaware, USA, device in order to analyze the volume phase transition temperature (*VPTT*). The swollen hydrogels in hermetic pans were scanned through heating and cooling runs from 15 to 50 °C at a heating/cooling rate of 3 °C min^{-1} and a nitrogen flow rate of 50 mL min^{-1}. Distilled water was used as the reference in the DSC measurements. DSC curves of hydrogels were analyzed by Universal Analysis 2000, version 4.1.0.16, software.

The viscoelastic properties of the NC hydrogels were studied using a mechanical spectrometer, model Discovery Hybrid Rheometer HR2 (TA Instruments). The hydrogels in both as-prepared and swollen state were analyzed, operating in the shear mode with parallel plate geometry. The diameter of the plates was 25 mm and gap of around 3 mm. The storage modulus, G', the loss modulus, G'', and the loss tangent, tan δ were analyzed as a function of frequency (0.1 to 100 rad s^{-1}) at 20 °C. Shear strain of 1 % was applied and it was established that the hydrogels were in the linear viscoelastic range at this strain.

RESULTS AND DISCUSSION

Synthesis and structure of NC hydrogels

In this study, three series of semi-IPN PNIPA hydrogels with linear water-soluble sodium salts of hyaluronic acid (Na-HA, Fig. 1) and one series of PNIPA hydrogels were synthesized by *in situ* free-radical redox polymerization in an aqueous suspension of the layered silicate, laponite XLG. The concentration of monomer NIPA in the reaction mixture was 1 mol dm^{-3}, corresponding to 10 wt. %. The clay content in the reaction mixture varied from 1 to 5 wt. %, while the Na-HA content was 0.1, 0.15 or 0.25 wt. %. The hydrogels were in the form of 2.5 mm thick sheets. The composition and some structural and physical properties of synthesized NC hydrogels in their as-prepared and equilibrium swollen states are given in Table I.

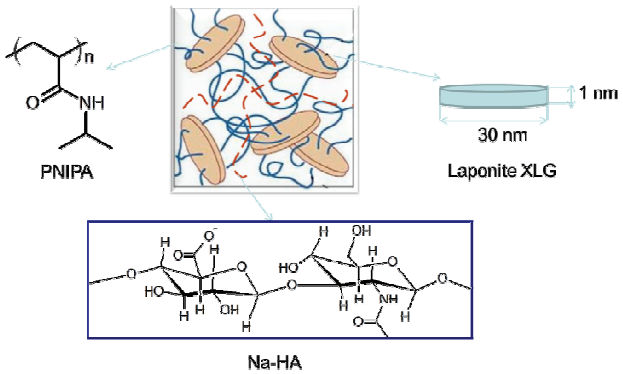

Fig. 1. Schematic representation of the NC hydrogel based on poly(*N*-isopropylacrylamide) (PNIPA), repeating disaccharide unit of sodium salts of hyaluronic acid (Na-HA) consisting of *N*-acetyl-D-glucosamine and D-glucuronic acid and nanoclay (laponite XLG).

The clay content in the NC xerogels was calculated from the residual weight at 770 °C estimated from TGA measurements. Assuming that the conversion of NIPA monomer to the cross-linked network is complete, the theoretical clay content in PNIPA-C xerogels ranged from 8.1 to 30.0 wt% and in SIPN series was between 7.4 and 29.8 wt%. When compared to the theoretical content of the clay in the reaction mixture, the results showed that the extent of the incorporation of clay in PNIPA hydrogels was in the range from 77 to 91 %, indicating loss of some laponite XLG particles from the gel network. In the series of SIPN hydrogels interpenetrated with 0.1 wt% Na-HA, the percent of the clay incorporation in the dried network was higher (99.5 to 114 %) in comparison to PNIPA series and in some cases higher than the theoretical one, probably due lower PNIPA monomer conversion. The notably higher quantity of laponite XLG clay remained in SIPN hydrogels, excluding a few exceptions (SIPN-HA0.15-C3, SIPN-HA0.25--C3), could be attributed to the presence of linear hydrophilic Na-HA, which suppresses extraction of laponite XLG particles from hydrogels. Similar observation was previously reported for PNIPA/PVP and PNIPA/PVA hydrogels.[13,14]

TABLE I. Composition and some structural and physical characteristics of the NC hydrogels in their as-prepared, equilibrium swollen and dried state

Sample	Content, wt. %				Q_e[d]	Average pore size[e], μm
	Na-HA[a]	Clay[b]	Clay in xerogel[c]	PNIPA in eq. swollen state		
PNIPA-C1	0	1	7.2 (88.6)	2.9	35.0	52.9±9.6
PNIPA-C3	0	3	19.2 (91.5)	5.4	18.4	22.0±12.9
PNIPA-C5	0	5	23.6 (76.9)	7.4	13.5	44.8±32.1
SIPN-HA0.1-C1	0.1	1	9.2 (114.1)	3.1	32.0	27.1±18.8
SIPN-HA0.1-C3	0.1	3	21.2 (101.8)	7.3	13.7	22.0±13.7
SIPN-HA0.1-C5	0.1	5	30.3 (99.4)	8.3	12.1	26.4±7.8
SIPN-HA0.15-C1	0.15	1	6.7 (83.4)	2.0	50.9	21.2±18.4
SIPN-HA0.15-C3	0.15	3	12.7 (61.3)	4.9	20.4	21.0±21.0
SIPN-HA0.15-C5	0.15	5	28.2 (92.8)	6.7	14.9	45.8±29.4
SIPN-HA0.25-C1	0.25	1	7.7 (96.6)	2.6	38.6	20.7±15.6
SIPN-HA0.25-C3	0.25	3	10.1 (48.8)	5.4	18.7	19.1±14.5
SIPN-HA0.25-C5	0.25	5	21.7 (71.8)	6.9	14.5	50.6±20.5

[a]Na-HA content in initial hydrogel (as-prepared); [b]clay content in initial hydrogel (as-prepared); [c]in parenthesis, percentage of incorporated clay relative to the added amount in NC xerogels; [d]equilibrium degree of swelling; [e]average pore size of freeze dried gels

The state of the dispersion of clay in the hydrogels was probed by XRD analysis, which was performed on the dried gel samples. The XRD patterns for Laponite XLG clay and powders of linear PNIPA and dried PNIPA and SIPN gel samples are presented in Fig. 2.

The characteristic peaks of the laponite XLG clay appear at 2θ 5.6 and 19.6 , attributed to a basal layer spacing of the clay platelets of 1.58 nm. In the diffrac-

tograms of the PNIPA samples, no reflection at $2\theta = 5.6°$ was observed, which points to intercalation or exfoliation of the clay in these xerogels. It was previously reported that the clay in NC gels could be extensively exfoliated and consequently, the clay platelets dispersed uniformly throughout the hydrogel sample.[5–7] The absence of this peak in difractograms of almost all SNIPA samples implies extensive intercalation or exfoliation. The only exception was noticed for the SNIPA samples SIPN-HA0.1-C3 and SIPN-HA0.1-C5 with higher amounts of clay and only 0.1 wt. % of Na-HA. In the difractograms of these samples, the reflection at 2θ between 2 and 3° (marked with arrows in Fig. 2a) shows intercalation of the clay with increase in basal spacing of the clay platelets to 3.8–4.0 nm. In the diffractogram of linear PNIPA (Fig. 2a), two broad reflections at 2θ around 7.7° (attributed to the aggregation of *N*-isopropyl groups in the PNIPA chains[35,36]) and 20° could be observed. These reflections are visible in the diffractograms of all NC samples and are superimposed on the diffraction of clay alone, at 2θ 19.6 . The diffraction peak of linear PNIPA slightly decreased with increasing clay content, while increased in the presence of linear Na-HA in all SIPN series.

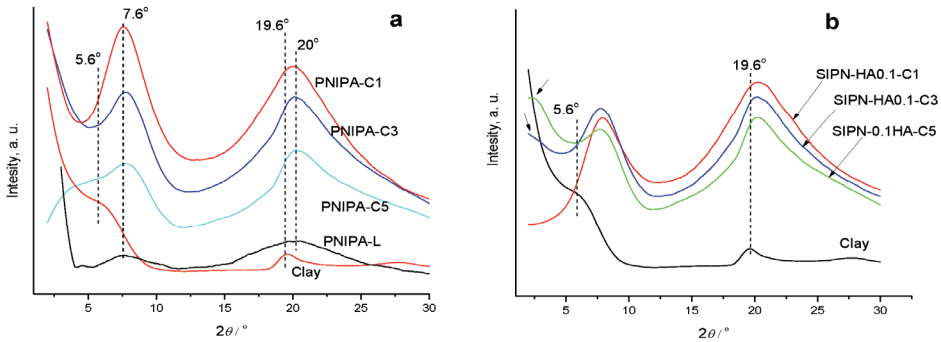

Fig. 2. XRD patterns of: a) XLG clay, linear PNIPA and PNIPA-C gels and b) SIPN gels with different contents of clay and 0.10 wt. % Na-HA.

Morphology of freeze-dried gels

The structural features of freeze-dried PNIPA and SIPN gels with linear Na-HA were analyzed by SEM. The SEM micrographs showing the morphology of the PNIPA hydrogels with different contents of the clay and linear penetrant, Na-HA are presented in Figs. 3 and 4. In order to preserve the porous hydrogel structure, freeze-drying was performed under the same preparation conditions. The SEM micrographs revealed that the SIPN and PNIPA gels had similar morphology characterized by a broad distribution of three-dimensional pores and very thin walls. The histogram of pore size distribution showed unimodal, broad distribution for all samples, Fig. 3. The pore sizes of the prepared PNIPA gels

were in the range from 22 to 53 μm and irregular, with standard deviations from 10 to 32 μm (Table I). The pore size of the SIPN networks decreased with addition of linear Na-HA in almost all cases, being 22 to 27 μm in the SIPN gels with 0.1 wt. % Na-HA. The sizes of pores as well as their size distributions are important morphological features since they control the kinetics of water diffusion in and out of the gel. It has been reported that the freeze-drying process could generate the honeycomb structure of the hydrogels, formed through hydrophobic interaction between polymer chains.[16,37]

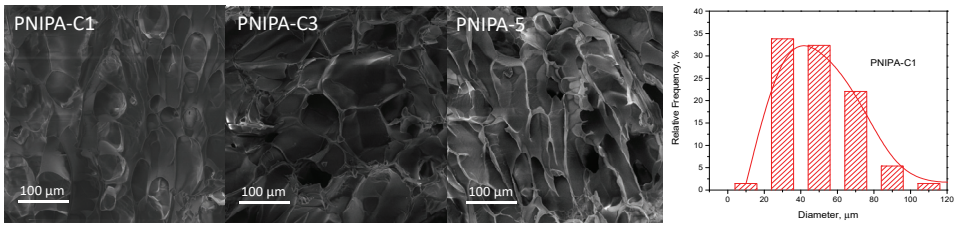

Fig. 3. SEM images of the freeze-dried PNIPA gels with different clay contents, 1, 3 and 5 wt. % (bar = 100 μm), and a representative histogram of the pore size distribution (PNIPA-C1).

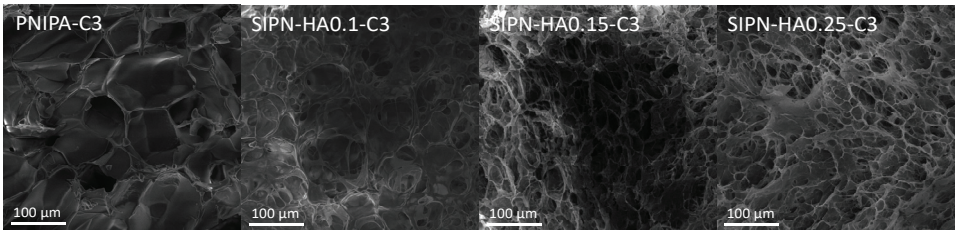

Fig. 4. SEM images of the freeze-dried PNIPA-C3 gel and SIPN-HA-C3 gels with different contents of HA (bar = 100 μm).

All the samples possessed a similar, highly irregular morphology, showing interconnected pores with thin walls and a very broad pore-size distribution. The pore size analysis revealed that the pore size of the hydrogel networks modestly changed in the presence of added linear Na-HA chains and changed more significantly with increasing the clay content, *i.e.*, in the PNIPA-C series.

All hydrogels consisted of areas with very wide channels and other areas with a large number of small pores. These networks are expected to exhibit a fast response to the temperature change, manifested as rapid volume shrinkage during the deswelling process. Additionally, numerous interconnected pores in SIPN networks and the smaller size of the pores should allow water molecules to diffuse easily, thus increasing the swelling and deswelling rates. The pore size of the SIPN-HAx-C5 networks increased slightly in the presence of added linear Na-HA chains, which is ascribed to the fact that a more expanded network could be generated in the SIPN hydrogels during swelling due to the increased hydro-

philicity. SIPN-HAx-C3 gels with higher degree of interconnected micro pores exhibited a faster swelling and deswelling rate, which is attributed to the presence of more channels for water diffusion in or out of the gels. In addition, with increasing clay content in the SIPN-HA0.1-Cx series, the pore diameter decreased slightly. The higher clay contents led to the formation of more densely cross-linked networks and thus, decreased the pore size of the gels, which affected the swelling/deswelling behavior of the hydrogels.

Swelling and dynamics of water swelling/deswelling of NC hydrogels

The equilibrium degrees of swelling (Q_e) of the PNIPA and SIPN hydrogels as function of the clay content and content of incorporated linear hydrophilic Na-HA in water at 25 °C are presented in Table I. The SIPN hydrogels had higher Q_e values in comparison to PNIPA hydrogels for almost all the samples, which ranged from 12.1 to 50.9 at temperatures below the *VPTT*. On the other hand, the Q_e values varied from 13.5 to 35.7 for PNIPA hydrogels. Hydrogels with 0.15 wt. % Na-HA exhibited the highest equilibrium degree of swelling (14.9–50.9), which was attributed to the lower incorporation of clay nanoparticles into the polymer network (based on TG analysis). The series of hydrogels with 0.25 wt. % HA displayed a slight drop in the equilibrium degree of swelling (14.5–38.6). The equilibrium degree of swelling was lower than that of the reference PNIPA series of hydrogels only in the series with 0.1 wt. % of Na-HA, as a result of the almost quantitative incorporation of nanoclays. In both the PNIPA and SIPN hydrogels, Q_e gradually decreased with increasing clay content, acting as a multifunctional cross-linker. The content of cross-linked PNIPA in the equilibrium swollen state varied in the range from 2.9 to 7.4 wt. %, whereas the concentration of semi-IPN polymer network including linear Na-HA was in the range from 2.0 to 8.3 wt. %, depending on the clay and Na-HA contents (Table I).

The swelling capacity is one of the most important properties of hydrogels. It was investigated in water at 25 °C by following the change in the degree of swelling with time (Fig. 5). Some of the samples, such as PNIPA-C3 and SIPN--HA0.15-C1 and SIPN-HA0.15-C5 exhibited the highest *SD* values, which could be attributed to the higher heterogeneity of their hydrogel structure (based on SEM). In addition, it could be seen that these *SD* values decreased with time (Figs. 5 and 6), and it could be envisaged that during time, the transport of water into and out of the hydrogels proceeds in a more regular manner. In general, NC hydrogels displayed higher swelling in water than chemically cross-linked hydrogels mainly because of their relatively low cross-linking density.[9] Dry PNIPA NC gels swelled quickly in the first 4 h, reaching equilibrium values in 2 to 4 days. Swelling of the SIPNs exhibited a similar trend but was initially slower, while a plateau was reached within 4 days. Slower swelling of hydrogels containing 0.1 wt.% Na-HA and lower Q_e displayed in Fig. 2, was attributed to the

higher cross-linking density and almost quantitative incorporation of the clays platelets into the polymer matrix. The lower initial rate of water absorption of SIPN NC hydrogels may be a consequence of hydrophobic interaction and reinforcing entanglement effects of the linear Na-HA interpenetrant with the PNIPA network, which restricted network expansion during the swelling process. One can envisage the dual role of the linear hydrophilic Na-HA, *i.e.*, in the first stage of swelling, the reinforcing effect of Na-HA dominates while in the second stage, its hydrophilicity governs.

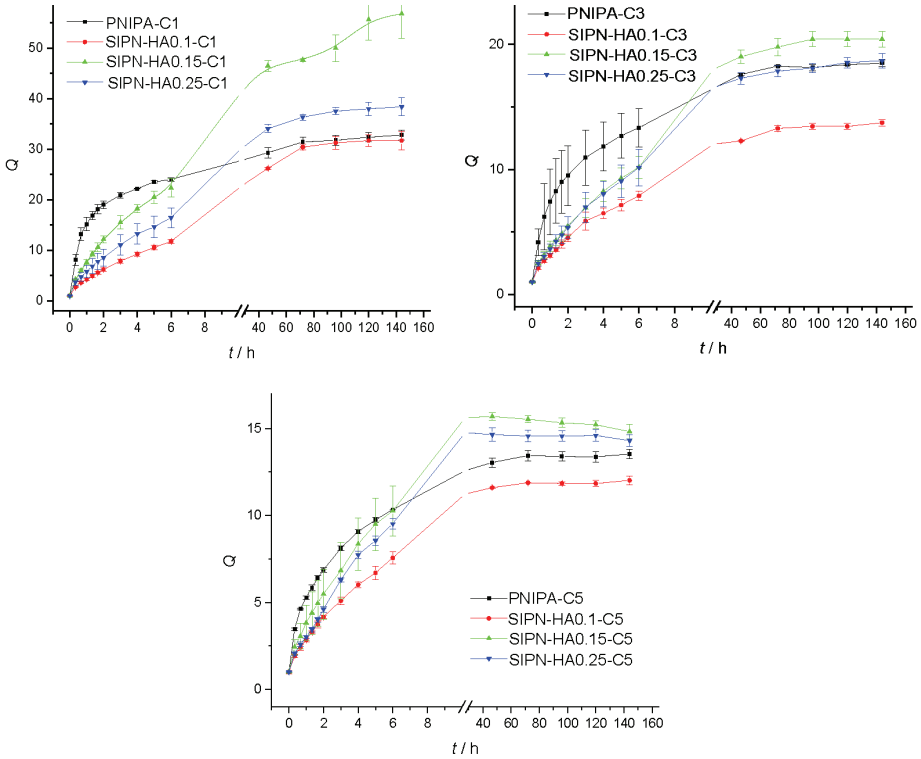

Fig. 5. The degree of swelling (Q) of the PNIPA and SIPN hydrogels with 1, 3 and 5 wt. % of clay and different Na-HA contents as a function of time at 25 °C.

The hydrogels containing linear hydrophilic Na-HA in amounts of 0.15 and 0.25 wt. % exhibited equilibrium degrees of swelling 1.02 to 1.4 times higher in comparison to pure PNIPA NC samples. Water sorption in the SIPN polymer networks was enhanced in the presence of hydrophilic anionic polyelectrolyte Na-HA at contents above 0.10 wt. %.

The swelling kinetics parameters of the NC hydrogels were calculated from the initial swelling rate, which was defined as $v_{in} = (Q–1)_{in}/t_{in}$ (where Q is the degree of swelling and t_{in} is time of sampling). It was calculated for the first 100

min and the results are presented in Table II. The thus-obtained initial swelling rates were 0.265, 0.165 and 0.081 min^{-1} for PNIPA-C1, PNIPA-C3 and PNIP--C5, respectively. The initial swelling rates of PNIPA NC hydrogels decreased with increasing clay content due to the higher cross-linking. A decrease in v_{in} with increasing clay content was observed for all SIPN hydrogels. SIPN hydrogels containing 0.15 wt% of hydrophilic Na-HA had v_{in} values of 0.119, 0.051 and 0.050 min^{-1} for SIPN-HA0.15-C1, SIPN-HA0.15-C3 and SIPN-HA0.15-C5, respectively. In addition, comparison of the initial swelling rates of SIPN and PNIPA hydrogels with the same clay content confirmed that the presence of the hydrophilic Na-HA did not have accelerating effect on the swelling kinetics. Among the SIPN samples, the series with 0.15 wt. % Na-HA exhibited faster swelling rates in the initial region and water uptake capability, mainly because of their relatively low cross-linking density.

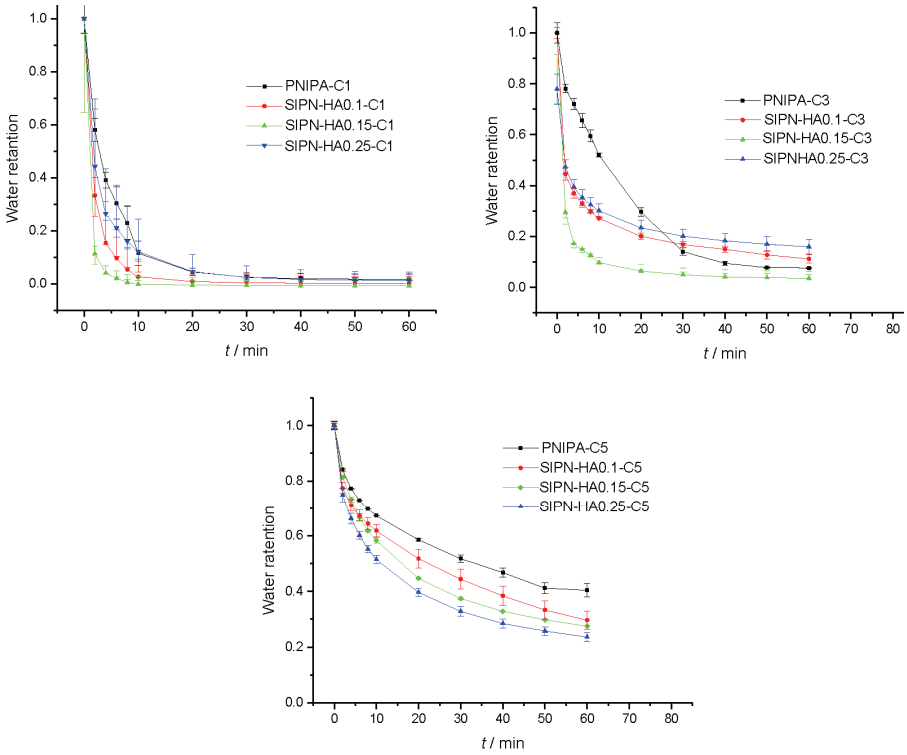

Fig. 6. Deswelling kinetics of the PNIPA and SIPN hydrogels with 1, 3 and 5 wt. % clay and different Na-HA content at 40 °C.

The isothermal kinetics of swelling of the NC hydrogels were investigated in order to obtain better insight into the effect of the hydrogel composition and mor-

phology on the water transport behavior. The nature of water diffusion into NC hydrogels was studied by fitting the initial water uptake data into Eq. (2):[38,39]

$$v_{\text{in}} = \frac{W(\text{H}_2\text{O})_t}{W(\text{H}_2\text{O})_\text{e}} = K\,t^n \tag{2}$$

where $W(\text{H}_2\text{O})_t$ and $W(\text{H}_2\text{O})_\text{e}$ are the weight of water absorbed by the hydrogel at time t and at the equilibrium swollen state, respectively. K is a constant characteristic for the structure of the hydrogel network and the solvent, and n is the diffusion or transport exponent. At $n < 0.5$, the swelling process is controlled by the Fickian diffusion mechanism. In cases where n ranges 0.5–1, the diffusion and relaxation of polymer chains control the swelling process (non-Fickian or anomalous diffusion).

TABLE II. Kinetics parameters for PNIPA and SIPN hydrogels evaluated from swelling/ /deswelling studies

Sample	Swelling			Deswelling		
	v_{in} / min^{-1}	K	n	R	k / min^{-1}	R
PNIPA-C1	0.265	0.0508	0.52	0.9500	0.1320	0.9785
PNIPA-C3	0.165	0.0337	0.57	0.9808	0.0670	0.9589
PNIPA-C5	0.081	0.0464	0.49	0.9940	0.0756	0,9693
SIPN-HA0.1-C1	0.060	0.0094	0.59	0.9933	0.3122	0.9925
SIPN-HA0.1-C3	0.039	0.0245	0.61	0.9980	0.0654	0.9100
SIPN-HA0.1-C5	0.033	0.0213	0.66	0.9940	0.0518	0.9752
SIPN-HA0.15-C1	0.119	0.0117	0.65	0.9981	0.4608	0.9153
SIPN-HA0.15-C3	0.051	0.0133	0.59	0.9957	0.2441	0.8301
SIPN-HA0.15-C5	0.050	0.0140	0.64	0.9920	0.0865	0.9640
SIPN-HA0.25-C1	0.088	0.0124	0.57	0.9890	0.2059	0.9227
SIPN-HA0.25-C3	0.048	0.0134	0.58	0.9888	0.1357	0.8727
SIPN-HA0.25-C5	0.037	0.0050	0.63	0.9918	0.0950	0.9345

In order to investigate the diffusion model for swelling NC hydrogels, the initial $(W(\text{H}_2\text{O})_t/W(\text{H}_2\text{O})_\text{e}) \leq 0.6$ swelling data were fitted to Eq. (2). The n and K values obtained from the slope and intercept of the plot of ln $(W(\text{H}_2\text{O})_t/W(\text{H}_2\text{O})_\text{e})$ *vs.* ln t are presented in Table II. The values of n for PNIPA NC hydrogels were around 0.5. A slight variation of diffusion exponent with increasing clay content was observed. The results pointed to non-Fickian or anomalous diffusion of water into the NC hydrogels, where the rates of water diffusion and polymer relaxation were comparable. The values of n for the SIPN hydrogels were around 0.6 and were independent of Na-HA or clay content. The current results are in agreement with previously reported values, that the water transport mechanism in NC hydrogels is non-Fickian diffusion, controlled by diffusion and macromolecular relaxation.[14,20]

For many applications, high rates of swelling/deswelling are a necessary requirement. The deswelling tests were performed by swelling to the equilibrium state at 25 °C (below *VPTT*) and then quickly switching to 40 °C (above *VPTT*).

The deswelling behavior of the NC hydrogels above phase transition temperature was studied by measuring the water retention for one hour, as shown in Fig. 6. The faster deswelling of SIPN compared to PNIPA hydrogels was due to the introduction of hydrophilic Na-HA chains. Lowering of deswelling rate with increasing clay content in both PNIPA and SIPN NC series was attributed to the highly cross-linked polymer network, which restricted collapse during the deswelling process. For instance, PNIPA hydrogels with 1 wt. % clay shrank and lost about 50 % of the water within 5 min, while the hydrogels with 3 and 5 wt. % clay lost 50 % of the water within 10 and 30 min, respectively. Deswelling was much faster for the SIPN hydrogels: the hydrogels interpenetrated with 0.1 to 0.25 wt. % Na-HA lost 50 and 75 % of water, respectively, in 2 min, while the PNIPA reinforced with same clay content (1 wt. %) lost only 40 %. Deswelling equilibrium was achieved within the 20 min for a series of SIPN with the lowest clay content (1 wt. %), while the other SIPN samples with the intermediate clay content (3 wt. %) required about 40 min and with the highest clay content (5 wt. %) more than one hour. It is well known that at temperatures above the *VPTT* of PNIPA hydrogels, the hydrophilic/hydrophobic balance in the surface region is destroyed and the hydrogels begin to collapse. Therefore, the deswelling process or collapsing is a diffusion controlled process that strongly depends on the gel size and structure. It was reported that hydrophilic polymer chains (PVA, PVP) in a SIPN network could act as water-releasing channels and disrupt the formation of a dense skin layer on the surface of hydrogels.[14,16] Considerably faster deswelling and volume shrinkage was obtained for SIPNs interpenetrated with 0.15 wt. % Na-HA. For the SIPN hydrogels, the influence of the Na-HA content was stronger than the content of clay. The introduction of Na-HA into NC hydrogels obviously improved the kinetics of the system, which opens up a possibility for broader application in controlled release systems with fast responsiveness.

To quantitatively analyze the deswelling process of NC hydrogels, first order kinetics was used, as follows:[20,39]

$$\ln \frac{m_t - m_D}{m_e - m_D} = -k\,t \tag{3}$$

where m_t, m_e and m_D are the weights of hydrogels at time t, in the equilibrium deswelling state and in the dried state, respectively, k is the deswelling rate constant and t is the deswelling time.

The linear plots of $\ln[(m_t–m_D)/(m_e–m_D)]$ *vs.* time for the hydrogels had high correlation coefficient values (Table II), indicating that the deswelling obey first--order kinetics.

In addition, the deswelling rate constants k was obtained from the slope of lines within range of the first 10 min. The deswelling rate constants are 0.132, 0.067 and 0.076 min^{-1} for the PNIPA reinforced with 1, 3 and 5 wt. % of clay, respectively. For the series of SIPN with clay content of 5 wt. %, the deswelling rate constants are: 0.052, 0.083 and 0.095 for the samples interpentrated with 0.1, 0.15 and 0.25 wt. % of Na-HA, respectively. It is clear that the deswelling rates of NC hydrogels in all series decreased with increasing clay content, as a consequence of higher cross-linking densities. SIPN hydrogels interpenetrated with 0.15 wt. % Na-HA exhibited faster deswelling. The positive effect of the presence of Na-HA on the deswelling of SIPNs as was previously discussed can be ascribed to its hydrophilicity. Besides the improvement of the response rate of NC hydrogels with the introduction of Na-HA, it is also possible to fine tune the deswelling kinetics with the amount of the clay and penetrant.

Thermal behavior of NC hydrogels

DSC analysis was used to study the transition temperatures and enthalpies of NC hydrogels in the equilibrium swollen state. DSC thermograms of the PNIPA series and SIPN NC hydrogels reinforced with 1 wt. % of clay and modified with different contents of Na-HA are shown in Fig. 7. The volume phase transition behavior of NC hydrogels in heating and cooling runs at a rate of 3 °C min^{-1} was evaluated. Peak onset temperatures (T_{onset}), peak maxima (T_{max}) and transition enthalpies (ΔH) are presented in Table III.

The temperature at the onset point of the DSC endothermic peak is referred to as the *VPTT* of the hydrogels. It was previously reported that the onset temperature (*VPTT*) was not affected by the clay content, whereas the peak profile became broader and shifted to higher temperatures as the clay content increased, due to increased hydrophilicity. The surfaces of the clay platelet are highly hydro-

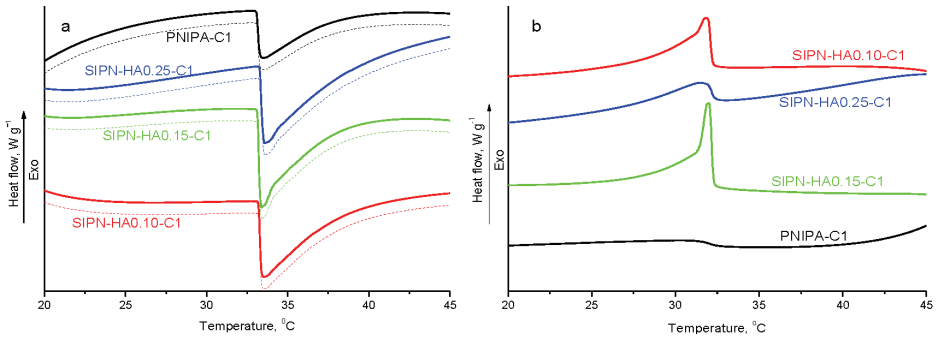

Fig. 7. DSC thermograms of PNIPA and SIPN NC hydrogels with 1 wt. % clay and different contents of Na-HA in the temperature range from 20 to 45 °C; a) heating I and II run (dashed line) and b) cooling run.

TABLE III. *VPTT* (T_{onset}), T_{max}, ΔH and *WHP* (width at half peak height) of phase transition of the NC hydrogels in their equilibrium swollen state during heating and cooling scans

Sample	Heating[a]					Cooling		
	T_{onset} °C	T_{max} °C	ΔH J g^{-1}	ΔH kJ mol^{-1}	*WHP* °C	T_{onset} °C	T_{max} °C	ΔH J g^{-1}
PNIPA-C1	33.1 (33.1)	33.5 (33.6)	1.3 (1.2)	5.0 (4.6)	2.8 (2.9)	32.6	30.5	0.5
PNIPA-C3	33.5 (33.8)	35.5 (34.8)	1.9 (1.9)	4.0 (4.1)	5.9 (4.4)	33.1	31.1	1.5
PNIPA-C5	33.7 (33.3)	36.3 (35.6)	1.0 (1.0)	1.5 (1.5)	5.1 (4.1)	33.4	31.3	0.6
SIPN-HA0.1-C1	33.2 (33.1)	33.5 (34.4)	2.5 (2.1)	8.8 (7.7)	2.8 (2.3)	32.2	31.8	1.4
SIPN-HA0.1-C3	33.2 (33.1)	34.2 (34.1)	2.6 (2.3)	4.1 (3.6)	3.8 (3.1)	32.3	31.6	1.3
SIPN-HA0.1-C5	33.7 (33.1)	36.3 (35.7)	0.8 (0.9)	1.2 (1.3)	4.5 (4.8)	33.6	31.3	1.1
SIPN-HA0.15-C1	33.1 (32.9)	33.4 (33.2)	2.5 (1.9)	13.9 (10.7)	2.9 (1.8)	32.2	32.0	1.6
SIPN-HA0.15-C3	33.4 (33.1)	33.7 (34.0)	2.0 (1.5)	4.5 (3.4)	3.2 (3.2)	32.4	31.6	0.8
SIPN-HA0.15-C5	33.7 (33.2)	37.2 (35.5)	1.4 (1.1)	2.3 (1.9)	5.0 (4.2)	33.4	31.4	1.1
SIPN-HA0.25-C1	33.3 (33.1)	33.6 (33.6)	2.3 (1.7)	10.3 (7.4)	3.1 (2.5)	32.3	31.3	0.7
SIPN-HA0.25-C3	33.3 (33.1)	35.4 (34.6)	1.4 (1.3)	3.0 (2.7)	5.5 (4.3)	32.6	31.6	1.4
SIPN-HA0.25-C5	33.5 (33.1)	36.5 (35.7)	0.8 (0.7)	1.4 (1.1)	5.7 (4.4)	33.3	31.0	0.6

[a]Data in the brackets were obtained in the second scan

philic and could interact with PNIPA chains through hydrogen bonding. The enthalpy of volume phase transition of PNIPA NC hydrogels decreased with increasing clay concentration.[40] The PNIPA NC hydrogels exhibited a *VPTT* of around 33 °C, in both the first and second heating runs. In the series of PNIPA hydrogels, DSC showed a shift of the temperatures of the endothermic peak maximum from 33.5 to 36.3 °C with increasing clay content. In addition, the width of DSC peaks at half peak height (*WHP*) increased with increasing clay content. These results indicate that the conformational change of the PNIPA chains from hydrated to dehydrated states in the NC hydrogels was largely suppressed by increased interaction between PNIPA chains and the clay platelets. This was also evident from the decrease in the transition enthalpy of PNIPA hydrogels with increasing clay content. For example, ΔH decreased from 5.0 to 1.5 kJ mol^{-1} in the series of PNIPA hydrogels with increasing clay content from 1 to 5 wt. %. The transition enthalpies of PNIPA hydrogels are in line with those of linear PNIPA chains in solution (about 5.0 kJ mol^{-1}).[35] The ΔH values in the second run were generally lower (by up to 28 %) compared to the values obtained in the first heating run due to hysteresis and slow relaxation of network chains.[4]

It is generally accepted that on addition of a hydrophilic component (such as co-monomer or linear polymer, interpenetrant) to PNIPA hydrogels, the hydrophilic/hydrophobic balance is shifted to a more hydrophilic nature and therefore the values of *VPTT* become higher.[26] The incorporation of the linear, highly hydrophilic Na-HA polymer into the PNIPA NC network slightly changed the *VPTT*, indicating that PNIPA network retains its own thermal sensitivity in semi-IPNs. On the other hand, the width at half peak height (*WHP*) of the transition

peak become larger with increasing clay content as well as on the introduction of the hydrophilic Na-HA. By comparing the values of enthalpy for the PNIPA and SIPN series with the corresponding clay content, it was observed that the enthalpies were significantly higher for the SIPN hydrogels only for those gels with low clay content (1 wt. %). The presence of hydrophilic Na-HA reduces the anchoring of PNIPA chains on the surface of the clay platelets, resulting in a decrease in the cross-linking density of the polymer network. Therefore, the coil--to-globule transition of the PNIPA chains was less suppressed in the presence of Na-HA. The sample SIPN-HA0.15-C1 exhibited the sharpest and narrowest DSC peak among all the SIPN and PNIPA hydrogels. In addition, the improved thermal response rates of the SIPN-HA0.15-C1 gel was confirmed by deswelling measurements, since the lower clay content and the presence of Na-HA could enable the formation of additional porosity.

Dynamic-mechanical analysis of NC hydrogels

Dynamic mechanical measurements were used to understand the effect of the structural constituents of the NC hydrogels, such as the contents of clay and Na-HA, on their viscoelastic properties. The DMA of the PNIPA and SIPNs NC hydrogels in the as-prepared and in the equilibrium swollen state were investigated in the shear mode at 25 °C. The rheological parameters, *i.e.*, the storage modulus (G'), loss modulus (G'') and loss factor ($\tan\delta = G''/G'$) of the PNIPA and SIPN NC hydrogels are given in Table IV. The frequency dependence of G', G'' and $\tan\delta$ for PNIPA NC series are presented in Fig. 8. The results showed that an increase in clay content from 1 to 5 wt. % resulted in an increase in G' from 1.9 to 14.2 kPa in the as-prepared gels due to an increase in the cross-linking densities of the network. As expected, the G' of the PNIPA hydrogels in the equilibrium swollen state decreased due to the lower concentration of chains per unit volume and ranged from 0.3 to 2.4 kPa. All PNIPA NC hydrogel samples

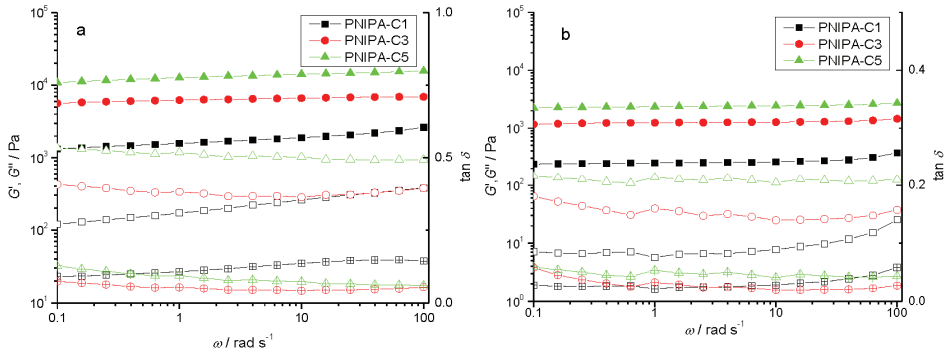

Fig. 8. Storage modulus G' (closed symbols) and G'' (open symbols) and tan δ (crossed open symbols) as a function of frequency for PNIPA-Cx (x = 1–3) hydrogels in the: a) as-prepared and b) equilibrium swollen state at 25 °C.

exhibited a storage modulus plateau over the measured frequency range, with the G' values always higher than the G'', indicating that the rubber elasticity of these hydrogels is controlled by the clay nanoparticles, acting as multifunctional cross--linkers. The linear increase in the shear modulus with increasing clay content indicated that clay nanoparticles were well-dispersed within the PNIPA matrix.[39]

TABLE IV. Dynamic mechanical properties and network parameters of the PNIPA and SIPN hydrogels in their as-prepared, swollen and dry state at 25 °C

Sample	As-prepared hydrogels[a]		Swollen hydrogels[b]		G' Pa[b]	G'_{red} kPa	N_e mol m^{-3}	$M_c \times 10^{-4}$ g mol^{-1}
	G' / kPa	tan δ	G' / kPa	tan δ				
PNIPA-C1	1.9	0.105	0.3	0.033	257	8.9	3.65	28.2
PNIPA-C3	6.7	0.053	1.3	0.023	1269	23.3	9.67	10.6
PNIPA-C5	14.2	0.077	2.4	0.041	2423	32.7	13.48	7.9
SIPN-HA0.1-C1	1.4	0.214	0.1	0.070	106	3.4	1.41	73.0
SIPN-HA0.1-C3	4.4	0.136	0.7	0.029	654	8.9	3.69	27.9
SIPN-HA0.1-C5	12.2	0.106	1.4	0.035	1379	16.7	6.84	15.1
SIPN-HA0.15-C1	1.9	0.210	0.08	0.075	81	4.1	1.68	61.3
SIPN-HA0.15-C3	5.2	0.173	0.3	0.066	277	5.6	2.33	44.2
SIPN-HA0.15-C5	17.1	0.105	1.9	0.052	1840	27.1	11.31	9.1
SIPN-HA0.25-C1	2.4	0.208	0.1	0.100	145	5.6	2.29	45.0
SIPN-HA0.25-C3	4.3	0.162	0.4	0.075	465	8.7	3.54	29.1
SIPN-HA0.25-C5	15.8	0.152	2.1	0.038	2095	30.4	12.51	8.2

[a]At 10 rad s^{-1}; [b]in swollen state at 0.1 rad s^{-1}

The frequency dependences of G', G'' and tan δ for three SIPN series reinforced with 0.1, 0.15 and 0.25 wt. % Na-HA and different contents of clay are shown in Fig. 9. A monotonic increase in the storage modulus with increasing clay content was also seen for these SIPN hydrogels. Almost all SIPN hydrogels exhibited lower values of G' in comparison to PNIPA NC with the same clay con- tent. The results revealed that the addition 0.1 wt. % of linear Na-HA decreased the elastic character of hydrogels. It is assumed that the presence of Na-HA weakened the hydrogel structure due to a decrease in the effective polymer network density. The changes in the storage modulus as a function of increasing amount of Na-HA and clay are illustrated in Fig. 10. The G' in NC hydrogels in the as-prepared state at the higher clay content (5 wt, %) increased with increasing Na-HA content, indicating a reinforcing effect of the linear interpenetrant of high molar mass. The decrease in G' of SIPN hydrogels reinforced with 3 wt.% of clay and containing 0.1 to 0.25 wt. % linear Na-HA, in the as-prepared state, was the most noticeable (Table IV). The weakening of hydrogel structure was observed in all cases in the swollen state, and was especially pronounced for the formulations with the lower clay content (1 and 3 wt. %).

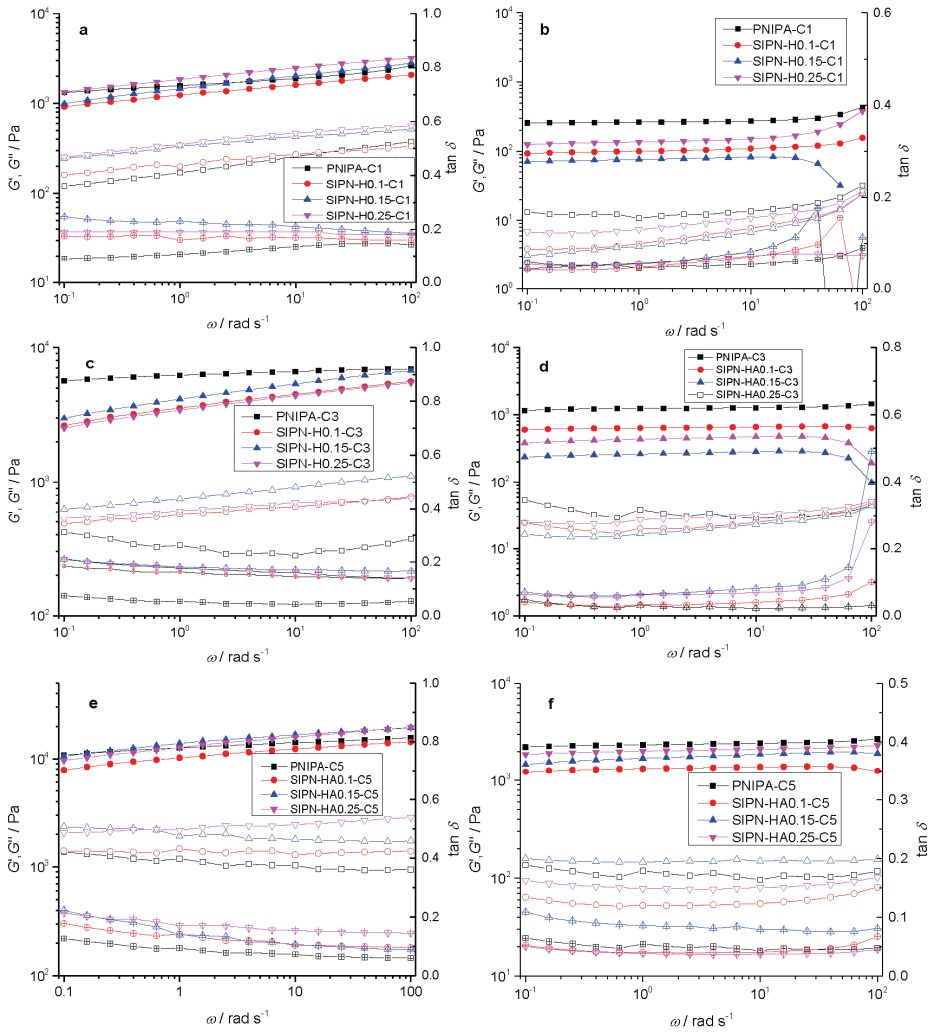

Fig. 9. Storage modulus G' (closed symbols) and G'' (open symbols) and tan δ (crossed open symbols) as a function of frequency of SIPN-HA*x*-C*y* (*x* = 0.1–0.25; *y* = 1–3) hydrogels in the as-prepared (a, c and e) and equilibrium swollen state (b, d and f).

The reduction of the storage modulus of SIPN hydrogels modified with hyaluronic acid (1, 2 and 3 wt. %) has been already reported.[26] It the case of NC hydrogels, this could be ascribed to an inhibiting effect of linear polymer on the polymerization process and decreased effective network chain density due to adsorption of Na-HA on the clay platelets. The adsorption of linear Na-HA chains on the clay platelets reduce the anchoring of PNIPA chains and therefore decrease their cross-linking effect in the NC hydrogels. Previously, Tong *et al.*[42] reported that due to the preferential adsorption of poly(ethylene glycol) (PEG)

chains on the laponite platelets in NC gels, the effective network density of the gels is reduced and therefore their mechanical properties and swelling behavior is changed.

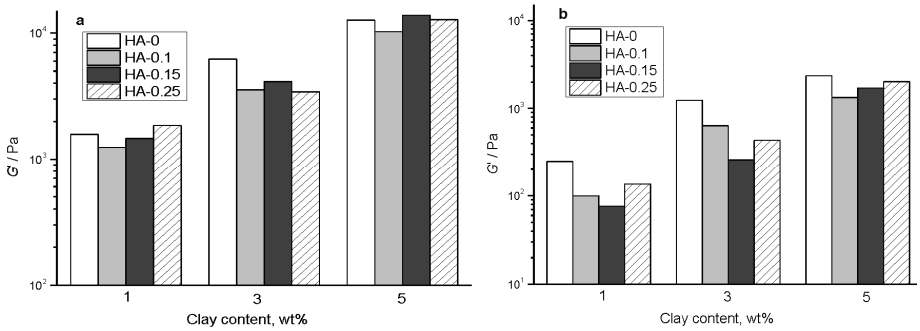

Fig. 10. Storage modulus G' (10 rad s^{-1}) of PNIPA and SIPN NC as a function of clay content and Na-HA content in the as-prepared (a) and equilibrium swollen state (b).

The values of loss factor, tan $\delta = G''/G'$, are presented in Table IV. It was reported previously that poly(acrylamide) NC hydrogels exhibited ten times larger tan δ (around 0.1) than the conventional chemically cross-linked hydrogels.[43] This confirms that the viscous component of NC hydrogels is more significant than in conventional hydrogels. For traditional chemically cross-linked hydrogels, tan δ is around 0.01, indicating well-developed and strong gel structure with negligible viscous response.

For the PNIPA hydrogels, tan δ decreases as the clay content increases from 1 to 3 wt. % due to the increased cross-linking density. However, for the highest clay content (5 wt. %) in both the as-prepared and equilibrium swollen state, the PNIPA NC hydrogels exhibited higher tan δ values, probably due to the increased amount of elastically ineffective chains. The introduction of Na-HA in the hydrogels led to an increase in tan δ for all SIPN samples, being especially pronounced for the lower clay contents (1 and 3 wt. %). The increased clay content in the SIPN series in the as-prepared state produced an expected decrease in the viscous response seen through the decrease of the corresponding tan δ values. The interpenetrant Na-HA produced the effect of increased viscous response in the samples with higher clay content (3 and 5 wt. %). All SIPN hydrogels have tan δ values ranging from 0.1 to 0.21 (Fig. 11). The same trends were also observed for all synthesized hydrogels in the equilibrium swollen state, exhibiting lower tan δ values.

The large tan δ values of PNIPA and SIPN hydrogels are related to a strong dissipation mechanism and indicate long relaxation times of polymer network chains in response to the external load. This could be one of the reasons for the excellent mechanical properties of the NC hydrogels reinforced with nanoclays.

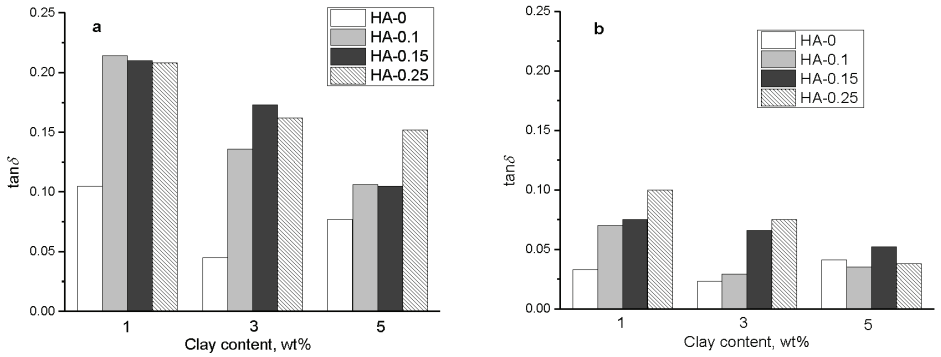

Fig. 11. Loss factor (tan δ at 10 rad s^{-1}) of PNIPA and SIPN NC as a function of clay content and Na-HA content in the as-prepared (a) and equilibrium swollen state (b).

In order to evaluate the effective network cross-linking density of PNIPA and SIPN NC hydrogels, the storage modulus values obtained for the lowest frequency or plateau were used. The effective network cross linking density, N_e of the hydrogels, assuming an affine network, are related to the equilibrium shear modulus G_e and can be evaluated using the following equation:[10,44]

$$G_e = \varphi \frac{\rho}{M_c} RT = N_e RT \quad (4)$$

where G_e was taken as the plateau modulus in the low frequency range of G' *vs.* ω curves, R and T are the gas constant and absolute temperature, respectively. The volume fraction, φ, of the polymer in the equilibrium swollen state was calculated as the reciprocal of the degree of swelling, M_c is the molar mass of network chains and ρ is the polymer density (1.03 g cm^{-3}). The estimated values of the effective network cross-linking density, N_e, and molar mass of network chains, M_c, and G'_{red} in the unswollen state (dried state) are summarized in Table IV. As the clay content increased from 1 to 5 wt. % in the PNIPA series, the effective cross-linking density N_e increased from 3.6 to 13.5 mol m^{-3} for gels in the unswollen state. Accordingly, as the clay content increased, the M_c decreased from 28.2×10^4 to 7.9×10^4 g mol^{-1}. Thus, the cross-linking efficiency and functionality of the nanoparticles increased as their content in the hydrogels increased. As expected, N_e increased with increasing clay content for all three SIPN hydrogel series. In addition, comparing the SIPNs and corresponding PNIPA hydrogels, it could be observed that the effective network cross-linking density N_e decreased with the introduction of Na-HA into the system because the Na-HA interactions with clay platelets surface could reduce the active sites for PNIPA chain anchoring, as was previously discussed. The values of M_c (from 8.2×10^4 to 73.0×10^4 g mol^{-1}) are large in SIPNs, implying that the polymer chains between clay sheets are long and flexible, adapting easily to macroscopic deformations. It

was shown that the chemically cross-linked PNIPA hydrogels with the higher network density and chain length around $M_c \approx 10^3$ g mol^{-1}, exhibited high fragility and therefore low mechanical properties.[12,45] However, the PNIPA hydrogels reinforced with nanoclays and the molar mass of the elastically active chains of $\approx 10^5$ g mol^{-1} exhibited high strength and good mechanical properties.

Finally, considering all properties of NC hydrogels in both as-prepared and swollen state, it was concluded that the hydrogel SIPN-HA0.15-C3, with 3 wt. % clay content and 0.15 wt. % of linear hydrophilic Na-HA displayed the best overall performance, including high swelling degree, fast deswelling rate and good dynamic mechanical properties.

CONCLUSIONS

Three series of semi-IPN hydrogels based on thermo-responsive PNIPA and Na-HA, as a linear interpenetrant, and reinforced with laponite XLG nanoclay were successfully prepared. The TG analysis indicated that one part of the clay was extracted from the hydrogels and a higher clay incorporation efficiency in the SIPN samples with a lower clay and Na-HA content. The XRD analysis revealed an exfoliated or extensively intercalated clay network structure in the dried NC gels, which were uniformly dispersed to clay platelets throughout the hydrogels during swelling. The quick thermal response was attributed to the porous honeycomb structure of the NC hydrogels as observed by SEM. The SIPN hydrogels, containing hydrophilic Na-HA exhibited higher Q_e values than the corresponding NC hydrogels, when the weight fraction of Na-HA exceeded 0.1 wt. %. The transport mode of water in both the PNIPA and SIPN NC hydrogels exhibited non-Fickian or anomalous diffusion, *i.e.*, it was controlled by water diffusion and the relaxation of the polymer chains. The deswelling rate decreased with increasing clay content and the highest values were obtained with 0.15 wt. % Na-HA. In both, the PNIPA and SIPN series, due to increased hydrophilicity, the endothermic peak of the phase transition become broader and shifted to higher temperature, while the enthalpy changes decreased with increasing clay content, as observed by DSC. In both the as prepared and equilibrium swollen state, the addition of clay (1 to 5 wt. %) increased the G' of the prepared PNIPA and SIPN hydrogels by 7 to 8 times. The presence of the anionic Na-HA reduced the values of G' and elastic character, indicating a weakening of the hydrogel networks in the swollen state and especially those with a lower clay content. The low effective cross-linking density (N_e) and the high values of M_c revealed that the polymer chains between the clay sheets are long and flexible, enabling large extensibility and toughness. These hydrogels are new nanomaterials with improved responsiveness, which, in combination with natural polymers, such as hyaluronic acid, may find application in biomedicine to create patches for rapid wound healing and tissue regeneration, as well as in the controlled release of drugs.

Acknowledgement. This work was financially supported by the Ministry of Education, Science and Technological Development of the Republic of Serbia (Project No. 172062).

ИЗВОД

ТЕРМИЧКИ-ОСЕТЉИВИ ХИДРОГЕЛОВИ НА БАЗИ ПОЛИ(*N*-ИЗОПРОПИЛ-АКРИЛАМИДА) И ХИЈАЛУРОНСКЕ КИСЕЛИНЕ УМРЕЖЕНИ НАНОГЛИНАМА

ИЛИНКА МИРКОВИЋ[1], МАРИЈА С. НИКОЛИЋ[1], САЊА ОСТОЈИЋ[2], ЈЕЛЕНА МАЛЕТАШКИЋ[3], ЗОРАН ПЕТРОВИЋ[4] и ЈАСНА ЂОНЛАГИЋ[1]

[1]Технолошко–металуршки факултет, Универзитет у Београду, Карнегијева 4, Београд, [2]Институт за општу и физичку хемију, Универзитет у Београду, Студентски трг 12–16, Београд, [3]Институт за нуклеарне науке Винча, Лабораторија за материјале, Универзитет у Београду, Београд и [4]Kansas Polymer Research Center, Pittsburg State University, Pittsburg, Kansas, 66762, USA

У оквиру овог рада су синтетисане семи-интерпенетрирајуће полимерне мреже (SIPN) на бази термички-осетљивог поли(N-изопропилакриламида) (PNIPA) и водорастворне соли хијалуронске киселине (Na-HA), физички умрежене синтетским наноглинама (laponite XLG). PNIPA хидрогелови различитог степена умрежености и концентрације Na-HA су синтетисани полимеризацијом преко слободних радикала у редокс систему. Структура и хетерогеност хидрогелова су анализирани помоћу електронске скенирајуће микроскопије (SEM) и рентгенске дифракције (XRD), док је садржај инкорпориране глине одређиван помоћу термогравиметријске анализе. DSC мерења су потврдила да се температуре запреминске фазне трансформације (*VPTT*) као и промене њихове енталпије мењају са додатком глине и линеарног полимера, Na-HA. SIPN хидрогелови, који садрже анјонски полиелектролит, Na-HA, имају веће равнотежне степене бубрења Q_e и брже се дехидратишу у односу на одговарајуће PNIPA нанокомпозитне хидрогелове. У присуству анјонског Na-HA полимера смањују се вредности модула сачуване енергије G' што указује на слабљење полимерне мреже хидрогелова, а нарочито је изражено код хидрогелова са мањим садржајем глине. Нанокомпозитни хидрогелови испољавају вискозни одговор, на што указују велике вредности tan δ, а који уједно расту са повећањем садржаја Na-HA.

(Примљено 9 јануара 2019, ревидирано 30 марта, прихваћено 2. маја 2020)

REFERENCES

1. N. A. Peppas, P. Bures, W. Leobandung, H. Ichikawa, *Eur. J. Pharm. Biopharm.* **50** (2000) 27 (https://doi.org/10.1016/S0939-6411(00)00090-4)
2. P. Calvert, *Adv. Mater.* **21** (2009) 743 (https://doi.org/10.1002/adma.200800534)
3. N. Annabi, A. Tamayol, J. A. Uquillas, M. Akbari, L. E. Bertassoni, C. Cha, G. Camci-Unal, M. R. Dokmeci, N. A. Peppas, A. Khademhosseini, *Adv. Mater.* **26** (2014) 85 (https://doi.org/10.1002/adma.201303233)
4. K. László, K. Kosik, E. Geissler, *Macromolecules* **37** (2004) 10067 (https://doi.org/10.1021/ma048363x)
5. K. Haraguchi, T. Takehisa, *Adv. Mater.* **14** (2002) 1120 (https://doi.org/10.1002/1521-4095(20020816)14:16<1120::AID-ADMA1120>3.0.CO;2-9)
6. K. Haraguchi, R. Farnworth, A. Ohbayashi, T. Takehisa, *Macromolecules* **36** (2003) 5732 (https://doi.org/10.1021/ma034366i)
7. K. Haraguchi, H.-J. Li, K. Matsuda, T. Takehisa, E. Elliott, *Macromolecules* **38** (2005) 3482 (https://doi.org/10.1021/ma047431c)
8. J. Nie, B. Du, W. Oppermann, *Macromolecules* **38** (2005) 5729 (https://doi.org/10.1021/ma050589s)

9. K. Haraguchi, T. Takehisa, S. Fan, *Macromolecules* **35** (2002) 10162 (https://doi.org/10.1021/ma021301r)
10. L. Xiong, X. Hu, X. Liu, Z. Tong, *Polymer* **49** (2008) 5064 (https://doi.org/10.1016/j.polymer.2008.09.021)
11. T. Wang, D. Liu, C. Lian, S. Zheng, X. Liu, Z. Tong, *Soft Matter.* **8** (2012) 774 (https://doi.org/10.1039/C1SM06484C)
12. J. Djonlagic, Z. S. Petrovic, *J. Polym. Sci., B* **42** (2004) 3987 (https://doi.org/10.1002/polb.20247)
13. J. Djonlagić, D. Žugić, Z. Petrović, *J. Appl. Pol. Sci.* **124** (2012) 3024 (https://doi.org/10.1002/app.35334)
14. J. Djonlagic, A. Lancuski, M. S. Nikolic, J. Rogan, S. Ostojic, Z. Petrovic, *J. Appl. Pol. Sci.* **134** (2017) 44535 (https://doi.org/10.1002/app.44535)
15. C. M. Paranhos, B. G. Soares, R. N. Oliveira, L. A. Pessan, *Macromol. Mater. Eng.* **292** (2007) 620 (https://doi.org/10.1002/mame.200700004)
16. J.-T. Zhang, R. Bhat, K. D. Jandt, *Acta Biomater*. **5** (2009) 488 (https://doi.org/10.1016/j.actbio.2008.06.012)
17. L. Song, M. Zhu, Y. Chen, K. Haraguchi, *Macromol. Chem. Phys*. **209** (2008) 1564 (https://doi.org/10.1002/macp.200800133)
18. J. Ma, B. Fan, B. Liang, J. Xu, *J. Colloid Interface Sci.* **341** (2010) 88 (https://doi.org/10.1016/j.jcis.2009.09.024)
19. J. Ma, Y. Xu, B. Fan, B. Liang, *Eur. Polym. J.* **43** (2007) 2221 (https://doi.org/10.1016/j.eurpolymj.2007.02.026)
20. J. Ma, L. Zhang, B. Fan, Y. Xu, B. Liang, *J. Polym. Sci., B* **46** (2008) 1546 (https://doi.org/10.1002/polb.21490)
21. J. Ma, Y. Xu, Q. Zhang, L. Zha, B. Liang, *Colloid Polym. Sci.* **285** (2007) 479 (https://doi.org/10.1007/s00396-006-1581-9)
22. M. A. Haq, Y. Su, D. Wang, *Mater. Sci. Eng., C* **70** (2017) 842 (https://doi.org/10.1016/j.msec.2016.09.081)
23. E. Fouissac, M. Milas, M. Rinaudo, *Macromolecules* **26** (1993) 6945 (https://doi.org/10.1021/ma00077a036)
24. M. K. Cowman, S. Matsuoka, *Carbohydr. Res.* **340** (2005) 791 (https://doi.org/10.1016/j.carres.2005.01.022)
25. M. D'Este, M. Alini, D. Eglin, *Carbohydr. Polym.* **90** (2012) 1378 (https://doi.org/10.1016/j.carbpol.2012.07.007)
26. R. Coronado, S. Pekerar, A. T. Lorenzo, M. A. Sabino, *Polym. Bull.* **67** (2011) 101 (https://doi.org/10.1007/s00289-010-0407-6)
27. J. R. Santos, N. M. Alves, J. F. Mano, *J. Bioact. Compat. Polym.* **25** (2010) 169 (https://doi.org/10.1177/0883911509357863)
28. A. R. Kim, S. L. Lee, S. N. Park, *Int. J. Biol. Macromol*. **118** (2018) 731 (https://doi.org/10.1016/j.ijbiomac.2018.06.061)
29. V. Capella, R. E. Rivero, A. C. Liaudat, L. E. Ibarra, D. A. Roma, F. Alustiza, F. Manas, C. A. Barbero, P. Bosch, C.R. Rivarola, *Heliyon* **5** (2019) 1 (https://doi.org/10.1016/j.heliyon.2019.e01474)
30. R. E. Rivero, V. Capella, A. C. Liaudat, P. Bosch, C. A. Barbero, N. Rodrigues, C. R. Rivarola, *RSC Adv*. **10** (2020) 5827 (https://doi.org/10.1039/C9RA08162C)
31. M. A. Cooperstaein, H. E. Canavan, *Biointerphases* **8** (2013) 19 (https://doi.org/10.1186/1559-4106-8-19)

32. Z. Guo, S. Li, C. Wang, J. Xu, B. Kirk, J. Wu, Z. Liu, W. Xue, *J. Bioact. Compat. Polym.* **32** (2017) 17 (https://doi.org/10.1177/0883911516648969)
33. L. H. Lima, Y. Morales, T. Cabral, *J. Ophthalmol.* (2016), Article ID 5356371 (https://doi.org/10.1155/2016/5356371)
34. S. Yogev, A. Shabtay-Orbach, A. Nyska, B. Mizrahi, *Toxicol. Pathol*. **47** (2018) 426 (https://doi.org/10.1177/0192623318810199)
35. K. Haraguchi, H.-J. Li, *Macromolecules* 39 (2006) 1898 (https://doi.org/10.1021/ma052468y)
36. Q. Zhang, L. Chen, Y. Dong, S. Lu, *Mater. Sci. Eng., C* **33** (2013) 1616 (https://doi.org/10.1016/j.msec.2012.12.096)
37. N. Kato, Y. Sakai, S. Shibata, *Macromolecules* **36** (2003) 961 (https://doi.org/10.1021/ma0214198)
38. P. L. Ritger, N. A. Peppas, *J. Control. Release* **5** (1987) 37 (https://doi.org/10.1016/0168-3659(87)90035-6)
39. Y. Xiang, Z. Peng, D. Chen, *Eur. Polym. J.* **42** (2006) 2125 (https://doi.org/10.1016/j.eurpolymj.2006.04.003)
40. K. Haraguchi, Y. Xu, *Colloid Polym. Sci.* **290** (2012) 1627 (https://doi.org/10.1007/s00396-012-2694-y)
41. K. Otake, H. Inomata, M. Konno, S. Saito, *Macromolecules* **23** (1990) 283 (https://doi.org/10.1021/ma00203a049)
42. X. Hu, T. Wang, L. Xiong, C. Wang, X.Liu, Z. Tong, *Langmuir* **26** (2010) 4233 (https://doi.org/10.1021/la903298n)
43. O. Okay, W. Oppermann, *Macomolecules* **40** (2007) 3378 (https://doi.org/10.1021/ma062929v)
44. C. Wu, S. Zhou, *Macromolecules* **30** (1997) 574 (https://doi.org/10.1021/ma960499a)
45. B. Strachota, M. Šlouf, J. Hodan, L. Matějka, *Colloid Polym. Sci.* **296** (2018) 753 (https://doi.org/10.1007/s00396-018-4289-8).